Structural, Spectroscopic and Thermodynamic Consequences of Anti-Chelate Effect in Nine-Coordinate Lanthanide Podates.

Patrick E. Ryan, Laure Guénée, Gabriel Canard, Frederic Gumy, Jean-Claude G. Bünzli and Claude Piguet*

Supporting Information

(15 pages)

Table S1 Bond Distances (δ_{ij}) Bond Valences (ν_{ij}, eq. 1) and Total Atom Valence (V_i, eq. 2) in the Crystal Structure of [Eu(**L10**)$_3$](ClO$_4$)$_3$.[30]

Atom [a]	Donor type	δ_{ij} / Å	ν_{ij}	
N1	Bzim	2.592	0.312	
N3	Py	2.576	0.326	
N4	Bzim	2.613	0.295	
N1'	Bzim	2.592	0.312	
N3'	Py	2.576	0.326	
N4'	Bzim	2.613	0.295	
N1"	Bzim	2.592	0.312	
N3"	py	2.576	0.326	Average N-heterocyclic
N4"	bzim	2.613	0.295	0.31(2)
		V_i	2.80	

[a] Numbering taken from reference 30.

Table S2 Bond Distances (δ_{ij}) Bond Valences (ν_{ij}, eq. 1) and Total Atom Valence (V_i, eq. 2) in the Crystal Structure of [Eu(**L12**)$_3$](ClO$_4$)$_3$.[29]

Atom [a]	Donor type	δ_{ij} / Å	ν_{ij}	
N1a	bzim	2.56	0.340	
N1b	bzim	2.66	0.260	
N1c	bzim	2.59	0.314	
N3a	py	2.60	0.305	
N3b	py	2.53	0.369	
N3c	py	2.56	0.340	
N4a	bzim	2.59	0.314	
N4b	bzim	2.61	0.297	Average N-heterocyclic
N4c	bzim	2.61	0.297	0.32(3)
		V_i	2.84	

[a] Numbering taken from reference 29.

Table S3 Bond Distances (δ_{ij}) Bond Valences (ν_{ij}, eq. 1) and Total Atom Valence (V_i, eq. 2) in the Crystal Structure of [Eu(**L9**)$_3$](ClO$_4$)$_3$.[27]

Atom [a]	Donor type	δ_{ij} / Å	ν_{ij}	
N1a	bzim	2.571	0.330	
N3a	py	2.553	0.347	
N4a	bzim	2.597	0.308	
N1b	bzim	2.614	0.294	
N3b	py	2.583	0.320	
N4b	bzim	2.631	0.281	
N1c	bzim	2.534	0.365	
N3c	py	2.559	0.341	Average N-heterocyclic
N4c	bzim	2.591	0.313	0.32(2)
		V_i	2.90	

[a] Numbering taken from reference 27.

Table S4 Crystal-Field Splitting Observed for Site I in [Eu(**L9**)$_3$](ClO$_4$)$_3$ (10 K, solid state, $\tilde{\nu}_{exc}$ = 25250 cm^{-1}).

Transitions	λ /nm	$\tilde{\nu}$ /cm^{-1}	Sublevel/cm^{-1}
$^5D_0 \rightarrow {}^7F_0$	580.8	17218	0
$^5D_0 \rightarrow {}^7F_1$	592.1	16889	329
	593.7	16844	374
	595.8	16784	434
$^5D_0 \rightarrow {}^7F_2$	612.3	16332	886
	616.0	16234	984
	618.9	16158	1060
	620.7	16111	1107
$^5D_0 \rightarrow {}^7F_3$	650.1	15382	1836
$^5D_0 \rightarrow {}^7F_4$	688.2	14531	2687
	689.4	14505	2713
	693.1	14428	2790
	697.0	14347	2871
	702.2	14241	2977
	708.3	14118	3100

Table S5 ^{1}H NMR Chemical Shifts (δ^{exp} /ppm with respect to $SiMe_4$) for **L9** in $CDCl_3$ and Its Complexes in CD_3CN at 298 K (Numbering in Chart 2).

Compd	H1	H2	H3	H4	H5	H6	H7	H8	H9
L9	0.77	1.43	2.29	3.81	7.74	7.30	7.37	8.36	7.99
[La(**L9**)]$^{3+}$	0.39	0.33	1.00 1.43	2.83 3.48	6.52	7.33	7.67	7.62	8.06
[Lu(**L9**)]$^{3+}$	0.41	0.36	0.98 1.48	2.79 3.47	6.29	7.34	7.67	7.59	7.94
[Y(**L9**)]$^{3+}$	0.40	0.35	0.99 1.48	2.80 3.47	6.35	7.34	7.66	7.59	7.96
[Ce(**L9**)]$^{3+}$	-0.23	-0.38 -0.08	-1.32 -0.92	2.19 3.14	3.46	7.18	8.05	8.77	9.08
[Pr(**L9**)]$^{3+}$	-1.04	-3.56 -2.27	-2.53 -1.92	1.48 2.73	-3.24	6.99	8.62	10.80	10.30
[Nd(**L9**)]$^{3+}$	-0.48	-2.15 -1.45	-1.03 -0.65	1.92 2.96	2.23	7.13	8.67	10.42	9.76
[Sm(**L9**)]$^{3+}$	0.26	-0.01 0.70	0.08 1.15	2.69 3.42	5.42	7.32	7.69	7.75	8.12
[Eu(**L9**)]$^{3+}$	1.23	2.08 2.77	2.97 3.46	3.72 4.02	11.58	7.55	6.03	3.57	5.93

Compd	H10	H11	H12	H13	H14	H15	H16	H17	H18
L9	8.36	7.33	7.18	7.64	4.73	1.33	4.73	1.33	2.52
[La(**L9**)]$^{3+}$	7.78	7.59	7.22	6.81	4.13 4.40	1.51	4.02 4.33	1.40	1.99
[Y(**L9**)]$^{3+}$	7.67	7.58	7.19	6.52	4.16 4.41	1.48	4.16 4.41	1.48	1.92
[Lu(**L9**)]$^{3+}$	7.66	7.59	7.19	6.42	4.19 4.49	1.50	4.19 4.49	1.50	1.91
[Ce(**L9**)]$^{3+}$	8.77	8.35	7.43	1.98	4.88 5.18	2.00	5.37 5.06	2.10	1.73
[Pr(**L9**)]$^{3+}$	10.60	9.26	7.62	-0.51	6.04 6.32	2.57	6.53 6.85	2.56	1.41

[Nd(**L9**)]$^{3+}$	10.26	9.02	7.46	0.65	5.35 5.85	2.15	5.70 6.20	2.32	1.56
[Sm(**L9**)]$^{3+}$	7.85	7.69	7.26	5.85	4.61 4.61	1.60	4.36 4.36	1.60	1.90
[Eu(**L9**)]$^{3+}$	4.05	5.62	7.03	10.75	2.77 2.97	0.90	2.25 2.51	0.68	2.42

Table S6 Nuclear Longitudinal Relaxation Times (T_{1i}^{exp} /s) Obtained for Protons H1, H5, H13, H15, H17 and H18 in the Complexes [Ln(**L9**)]$^{3+}$ (CD_3CN, 298 K).

Compd	H1	H5	H13	H15	H17	H18
[La(**L9**)]$^{3+}$	2.88E-01	1.04E+00	1.93E+00	5.07E-01	5.05E-01	6.14E-01
[Lu(**L9**)]$^{3+}$	3.02E-01	1.00E+00	1.87E+00	4.51E-01	4.51E-01	6.50E-01
[Ce(**L9**)]$^{3+}$	2.92E-01	7.30E-02	1.14E-01	3.86E-01	3.95E-01	4.74E-01
[Pr(**L9**)]$^{3+}$	2.86E-01	3.09E-02	3.55E-02	3.30E-01	3.09E-01	3.65E-01
[Nd(**L9**)]$^{3+}$	2.76E-01	1.74E-02	3.23E-02	2.37E-01	nd[a]	2.72E-01
[Sm(**L9**)]$^{3+}$	2.95E-01	2.04E-01	2.56E-01	4.62E-01	4.62E-01	5.72E-01
[Eu(**L9**)]$^{3+}$	2.78E-01	4.71E-02	5.48E-02	3.38E-01	3.44E-01	4.09E-01
[Tb(**L9**)]$^{3+}$	8.22E-02	5.37E-04	6.49E-04	1.33E-02	1.35E-02	1.47E-02
[Dy(**L9**)]$^{3+}$	7.51E-02	4.65E-04	5.36E-04	1.09E-02	1.13E-02	1.25E-02
[Ho(**L9**)]$^{3+}$	8.39E-02	3.99E-04	6.82E-04	1.53E-02	1.43E-02	1.49E-02
[Tm(**L9**)]$^{3+}$	1.95E-01	1.97E-03	2.20E-03	4.72E-02	4.59E-02	4.53E-02
[Yb(**L9**)]$^{3+}$	2.10E-01	1.10E-02	1.24E-02	2.08E-01	2.09E-01	2.16E-01

[a] Not determined because of overlap with the residual peak of water.

Table S7 Polar Axial Coordinates r_i and θ_i of the Protons H1, H5, H13, H15, H17 and H18 in the Principal Magnetic Axes System in the Crystal Structure of [Eu(**L9**)]$(ClO_4)_3$.[a]

	Strand A		Strand B		Strand C	
Protons	r_i /Å	θ_i /°	r_i /Å	θ_i /°	r_i /Å	θ_i /°
H1	8.83	7.39	8.83	7.39	8.83	7.39
	9.05	3.03	9.05	3.03	9.05	3.03
	8.77	8.16	8.77	8.16	8.77	8.16
H5	3.96	33.1	4.00	35.6	3.79	39.6
H13	3.97	143.8	4.08	122.6	4.05	146.1
H15	7.08	54.3	6.87	55.3	5.64	97.9
	6.67	57.2	6.32	62.9	6.07	96.1
	7.65	64.2	7.59	66.1	7.09	93.7
H17	7.18	117.0	7.19	104.6	7.02	122.7
	6.71	112.3	6.73	105.4	6.60	120.0
	7.73	106.5	7.75	96.8	7.54	112.5
H18	7.02	142.5	7.13	120.5	7.14	141.2
	6.16	132.0	6.25	111.2	6.18	131.7
	7.29	129.2	7.39	107.3	7.17	127.9

[a] The *z* axis coincides with the pseudo-threefold axis passing through the Eu atom and the capping quaternary atom of the tripod and Eu(III) is located at the origin (Figure 2c).

Table S8 Experimental Paramagnetic ^{1}H NMR Chemical Shifts (δ^{para} /ppm, Eq 7) for Protons H1, H5, H13, H15, H17 and H18 in [Ln(**L9**)]$^{3+}$ (CD_3CN, 298 K).[a]

Compd	H1	H5	H13	H15	H17	H18
[Ce(**L9**)]$^{3+}$	-0.62	-3.06	-4.83	0.49	0.70	-0.26
[Pr(**L9**)]$^{3+}$	-1.43	-9.76	-7.32	1.06	1.16	-0.58
[Nd(**L9**)]$^{3+}$	-0.87	-4.29	-6.16	0.64	0.92	-0.43
[Sm(**L9**)]$^{3+}$	-0.13	-1.10	-0.96	0.09	0.20	-0.09
[Eu(**L9**)]$^{3+}$	0.84	5.06	3.94	-0.61	-0.72	0.43
[Tb(**L9**)]$^{3+}$	-6.94	-41.64	-53.21	5.35	7.76	-2.23
[Dy(**L9**)]$^{3+}$	-10.52	-72.29	-58.42	7.51	10.43	-3.54
[Ho(**L9**)]$^{3+}$	-7.58	-54.75	-44.85	5.33	7.14	-3.04
[Tm(**L9**)]$^{3+}$	3.05	20.69	17.72	-2.32	-3.78	1.14
[Yb(**L9**)]$^{3+}$	1.79	11.28	9.57	-1.25	-1.87	0.64

[a] See chart 2 for the atom-numbering scheme.

Table S9 Computed Paramagnetic ^{1}H NMR Chemical Shifts ($\delta^{para,calcd}$ /ppm, Eq 14, F_i and $B_0^2G_i$ Taken from Table 2) for Protons H1, H5, H13, H15, H17 and H18 in [Ln(**L9**)]$^{3+}$ (CD_3CN, 298 K).[a]

Compd	H1	H5	H13	H15	H17	H18
[Ce(**L9**)]$^{3+}$	-0.77	-5.36	-4.01	0.58	0.69	-0.31
[Pr(**L9**)]$^{3+}$	-1.39	-9.64	-7.23	1.04	1.25	-0.58
[Nd(**L9**)]$^{3+}$	-0.68	-4.42	-3.38	0.50	0.61	-0.31
[Sm(**L9**)]$^{3+}$	-0.08	-0.56	-0.41	0.06	0.07	-0.03
[Eu(**L9**)]$^{3+}$	0.92	5.63	4.41	-0.67	-0.83	0.47
[Tb(**L9**)]$^{3+}$	-9.23	-66.47	-53.36	6.73	9.39	-3.19
[Dy(**L9**)]$^{3+}$	-9.83	-70.14	-56.58	7.19	10.18	-3.39
[Ho(**L9**)]$^{3+}$	-5.05	-37.08	-29.51	3.67	4.97	-1.76
[Tm(**L9**)]$^{3+}$	2.73	17.43	14.87	-2.06	-3.37	0.90
[Yb(**L9**)]$^{3+}$	1.22	7.93	6.70	-0.92	-1.47	0.41

[a] See chart 2 for the atom-numbering scheme.

Table S10 Computed Paramagnetic ^{1}H NMR Pseudo-Contact Shifts (δ^{pc} /ppm, Eq 7, F_i Taken from Table 2 and δ^{c} Calculated with Eq 8) for Protons H1, H5, H13, H15, H17 and H18 in [Ln(**L9**)]$^{3+}$ (CD_3CN, 298 K).[a]

Compd	H1	H5	H13	H15	H17	H18
[Ce(**L9**)]$^{3+}$	-0.58	-2.85	-4.65	0.46	0.66	-0.23
[Pr(**L9**)]$^{3+}$	-1.30	-9.11	-6.76	0.97	1.04	-0.50
[Nd(**L9**)]$^{3+}$	-0.68	-3.31	-5.31	0.51	0.74	-0.31
[Sm(**L9**)]$^{3+}$	-0.13	-1.11	-0.97	0.09	0.20	-0.09
[Eu(**L9**)]$^{3+}$	0.38	2.73	1.93	-0.29	-0.30	0.14
[Tb(**L9**)]$^{3+}$	-3.56	-18.65	-28.67	2.96	5.00	-1.01
[Dy(**L9**)]$^{3+}$	-7.49	-51.66	-36.40	5.37	7.95	-2.44
[Ho(**L9**)]$^{3+}$	-5.18	-38.40	-27.40	3.63	5.17	-2.17
[Tm(**L9**)]$^{3+}$	3.92	26.62	24.05	-2.94	-4.49	1.46
[Yb(**L9**)]$^{3+}$	2.06	13.15	11.57	-1.44	-2.09	0.74

[a] See chart 2 for the atom-numbering scheme.

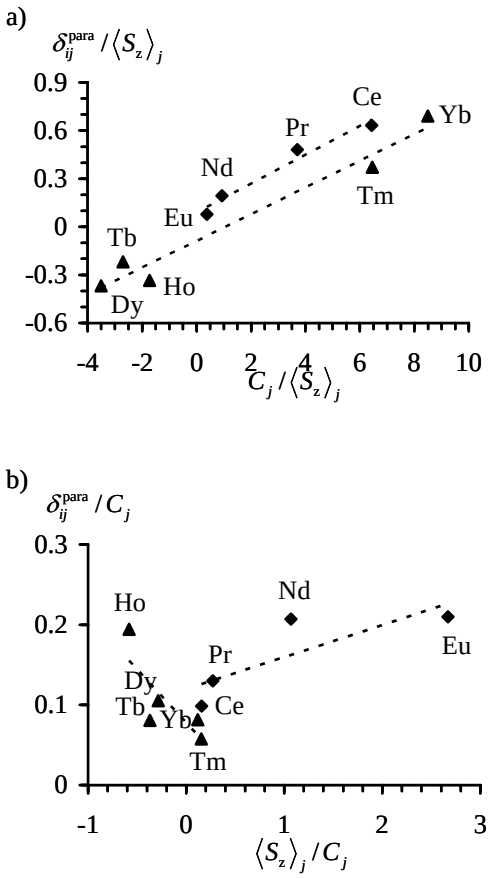

Figure S1 Plots of a) $\delta_{ij}^{para} / \langle S_z \rangle_j$ *vs* $C_j / \langle S_z \rangle_j$ and b) δ_{ij}^{para} / C_j *vs* $\langle S_z \rangle_j / C_j$ for protons H1 in [Ln(**L9**)]$^{3+}$ (CD_3CN, 298 K, Ln = Ce-Yb, except Pm, Gd and Er, Sm is not shown because of its faint paramagnetism).

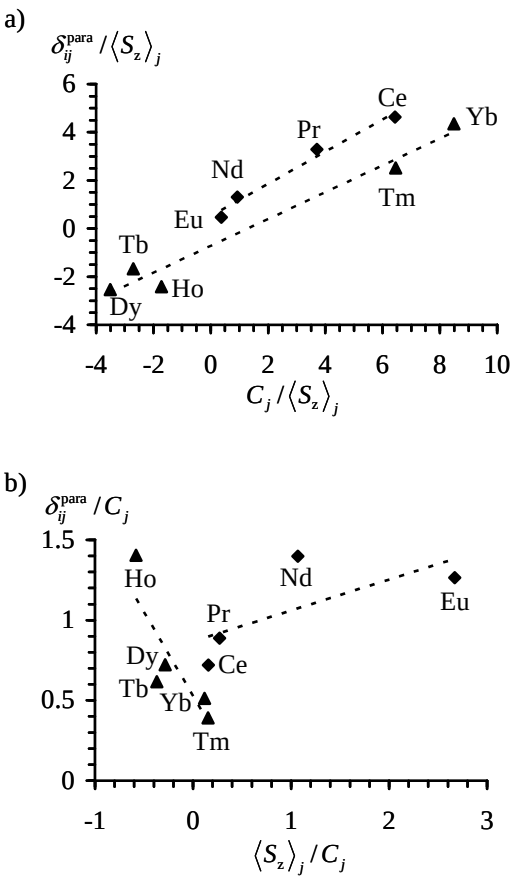

Figure S2 Plots of a) $\delta_{ij}^{para}/\langle S_z\rangle_j$ *vs* $C_j/\langle S_z\rangle_j$ and b) δ_{ij}^{para}/C_j *vs* $\langle S_z\rangle_j/C_j$ for protons H5 in [Ln(**L9**)]$^{3+}$ (CD_3CN, 298 K, Ln = Ce-Yb, except Pm, Gd and Er, Sm is not shown because of its faint paramagnetism).

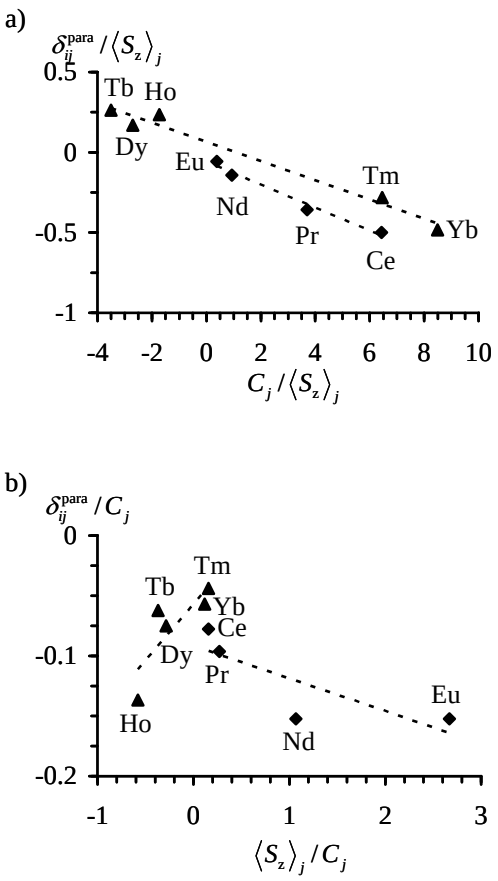

Figure S3 Plots of a) $\delta_{ij}^{para}/\langle S_z\rangle_j$ *vs* $C_j/\langle S_z\rangle_j$ and b) δ_{ij}^{para}/C_j *vs* $\langle S_z\rangle_j/C_j$ for protons H15 in [Ln(**L9**)]$^{3+}$ (CD_3CN, 298 K, Ln = Ce-Yb, except Pm, Gd and Er, Sm is not shown because of its faint paramagnetism).

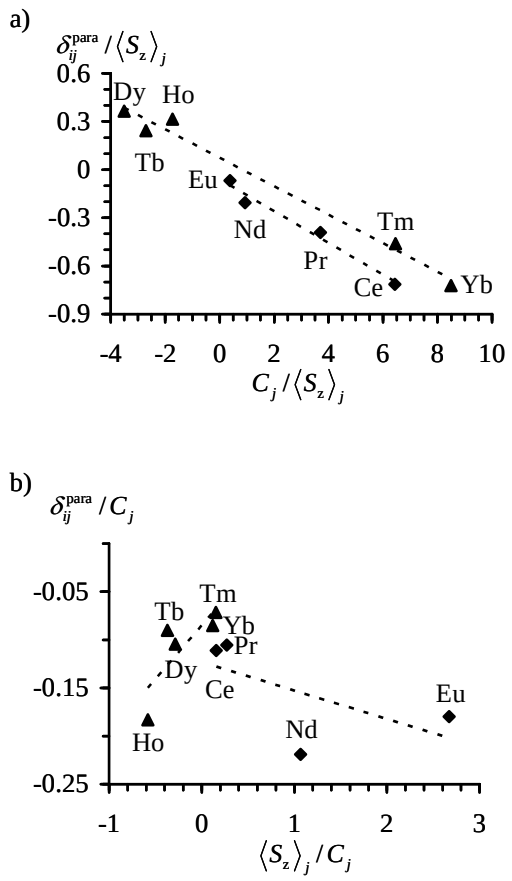

Figure S4 Plots of a) $\delta_{ij}^{para}/\langle S_z\rangle_j$ *vs* $C_j/\langle S_z\rangle_j$ and b) δ_{ij}^{para}/C_j *vs* $\langle S_z\rangle_j/C_j$ for protons H17 in [Ln(**L9**)]$^{3+}$ (CD_3CN, 298 K, Ln = Ce-Yb, except Pm, Gd and Er, Sm is not shown because of its faint paramagnetism).

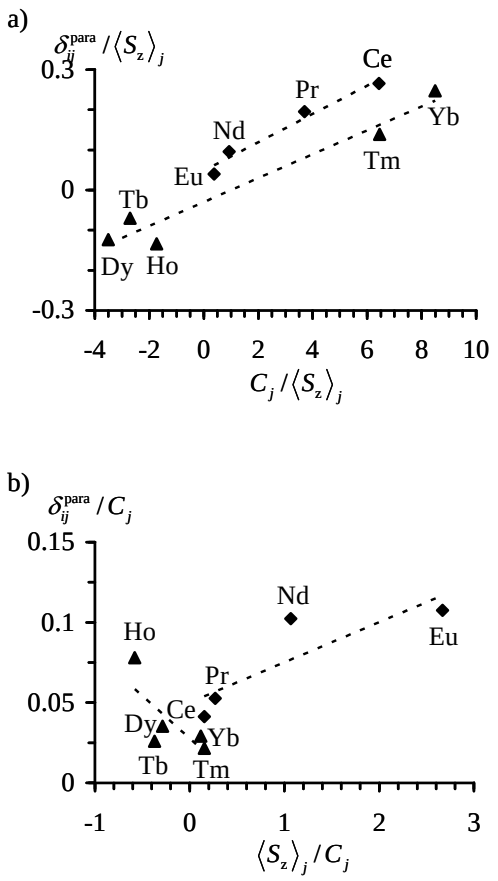

Figure S5 Plots of a) $\delta_{ij}^{para}/\langle S_z\rangle_j$ *vs* $C_j/\langle S_z\rangle_j$ and b) δ_{ij}^{para}/C_j *vs* $\langle S_z\rangle_j/C_j$ for protons H18 in [Ln(**L9**)]$^{3+}$ (CD_3CN, 298 K, Ln = Ce-Yb, except Pm, Gd and Er, Sm is not shown because of its faint paramagnetism).